

# Co-Sedimentation of TiO<sub>2</sub> Nanoparticles and Polymer Beads to Fabricate Macroporous TiO<sub>2</sub> Photoelectrodes

Min-A Kim<sup>1</sup>, Young Gon Seo<sup>1,2</sup>, Sang-Soo Lee<sup>1</sup>, Wonmok Lee<sup>2,\*</sup>,†, and Hyunjung Lee<sup>3,\*</sup>,†

<sup>1</sup>Hybrid Materials Research Center, Korea Institute of Science and Technology, Seoul 136-791, Republic of Korea

<sup>2</sup>Department of Chemistry, Sejong University, 98 Gunja-Dong, Gwangjin-Gu, Seoul 143-747, Republic of Korea

<sup>3</sup>School of Advanced Materials Engineering, Kookmin University, Jeongneung-Dong, Seoul, 136-702, Republic of Korea

Dye-sensitized solar cells based on highly porous nanocrystalline TiO<sub>2</sub> films have drawn considerable attention due to their high conversion efficiency and low production cost. TiO<sub>2</sub> nanocrystalline electrodes have been investigated extensively as a key material. In this study, we discuss dye-sensitized solar cells based on macroporous TiO<sub>2</sub> films using a highly-dispersed aqueous solution of TiO<sub>2</sub> nanoparticles and polymeric particles. After drying this solution on the conducting glass substrate, the sacrificial polymer particles were removed selectively by thermal sintering at high temperatures over 400 °C or chemical treatment at the low temperature of 150 °C. This method provides the flexible control of TiO<sub>2</sub> fractions or pore size or fabrication temperature. Also highly-dispersed TiO<sub>2</sub> particles with a high crystallinity would provide a promising solution on low-temperature process for flexible DSSCs.

**Keywords:** Dye-Sensitized Solar Cells, Macroporous TiO<sub>2</sub> Films, Low Temperature Process, Highly Dispersed TiO<sub>2</sub> Solution, Polymer Microspheres.

## 1. INTRODUCTION

Dye-sensitized solar cells (DSSCs) based on highly porous nanocrystalline TiO<sub>2</sub> films have drawn considerable attention due to their high conversion efficiency and low production cost. TiO<sub>2</sub> nanocrystalline electrodes have been investigated extensively as a key material. Conventional TiO<sub>2</sub> electrodes have a large surface area, but their randomly connected structure is a limiting factor for solid type electrolytes and random electron transfer paths. In recent studies, there have been a lot of approaches to obtain the modified nanostructured materials with various morphologies such as nanoparticles, nanorods, nanowires, and inverse opal structures.<sup>1–3</sup> Also, solid state DSSCs have been suggested as a promising candidate using viscous polymer gels or solid materials because they provide long term stability for outdoor uses and stable outputs.<sup>4</sup> High-temperature processes produce high performance DSSCs, but lightweight and flexible DSSCs have not been achieved. Recently, flexible DSSCs have been developed in which the typical fluorine-doped tin oxide

(FTO) glass substrate is replaced with a conductive polymeric substrate, such as poly(ethylene terephthalate) or poly(ethylene naphthalate) coated with indium-doped tin oxide (ITO/PET or ITO/PEN).<sup>5,6</sup> Lightweight, flexible, and low cost DSSCs on conductive polymeric substrates have attracted considerable interest due to their potential applications as photovoltaic power supplies, including their uses in mobile electronic devices. Therefore, the development of low-temperature (<150 °C) processes is necessary for flexible devices.

Typically, a low-temperature fabrication of TiO<sub>2</sub> nanocrystalline films results in poor interconnection among TiO<sub>2</sub> particles and poor substrate adhesion. This may lead to an increase of interfacial resistance in electron transport, producing poor cell performance. Recently, many research groups have tried to develop various experimental methods for low-temperature process such as binderless low-temperature annealing, chemical treatment with the addition of ammonia, mechanical compression, electrophoretic deposition, transfer composite layer, hydrothermal crystallization, and so on.<sup>7–13</sup> It was found that the absence of organic additives such as polymers or surfactants yielded a better adhesion onto a substrate and a

\*Authors to whom correspondence should be addressed.

†H. Lee and W. Lee contributed equally to this work.

increased adsorption of more dye molecules in TiO<sub>2</sub> electrodes treated at low-temperature.

Lee et al. have reported the novel fabrication of a TiO<sub>2</sub> photoelectrode having submicron-sized pores, which was fabricated using polymeric colloidal templates, which were decomposed by thermal treatment at high temperature (>400 °C).<sup>14</sup> If polymer particles are removed at low temperature, the polymer template method will provide a promising solution as a low-temperature process for flexible DSSCs. In order to overcome several issues for low-temperature process, we used highly dispersed TiO<sub>2</sub> nanoparticles in water and prepared a mixed aqueous solution of TiO<sub>2</sub> nanoparticles and polymer particles. In order to increase the crystallinity and dispersibility in water of TiO<sub>2</sub> nanoparticles, we used hydrothermal synthesis and peptization process.<sup>15,16</sup> The polymeric particles are removed selectively by thermal or chemical processes.

## 2. FIRST-ORDER HEADING

### 2.1. Highly Dispersed TiO<sub>2</sub> Nanocrystalline Particles in Water

The homogeneous mixture of PS microspheres and TiO<sub>2</sub> nanoparticles is necessary in the co-sedimentation method. In this study, a highly stable TiO<sub>2</sub> suspension in water was obtained by the peptization process, in which the aggregation of TiO<sub>2</sub> nanoparticles can be minimized and the crystallinity can be increased by introducing various peptizing agent. The detailed synthesis method was described elsewhere.<sup>17,18</sup> Following peptization, the suspension was autoclaved to allow the growth of the nanoparticles to the desired size. This autoclaving step was controlled both by the temperature and the pH conditions employed in the preceding peptization. The size and crystallinity of the synthesized TiO<sub>2</sub> nanoparticles used in this study was revealed as anatase by transmission electron microscopy (TEM) and X-ray diffraction (XRD) analysis, as shown in Figure 1. Figure 1(a) shows a lattice image of 3.45 Å that is clearly observable, corresponding to the (101) planes of TiO<sub>2</sub> anatase phase. Figure 1(b) shows the typical XRD pattern recorded for the TiO<sub>2</sub> nanoparticles before and after a hydrothermal reaction. Several characteristic diffraction peaks develop sharply with high intensity due to the high crystallinity generated during the hydrothermal reaction. They correspond to anatase (101), (200), and (105) morphology showing up at  $2\theta = 25.2^\circ$ ,  $48^\circ$ , and  $54^\circ$ , respectively. TEM images show that the average particle size of peptized TiO<sub>2</sub> ranges between 30–40 nm. The compatible P25 (Degussa) particle size is known to be approximately 15–20 nm. Even though P25 dispersions exhibit a turbid white solution due to the existence of aggregates, the peptized TiO<sub>2</sub> particles showed a highly-dispersed translucent solution.

### 2.2. Fabrication of Solar Cells Using the Co-Sedimentation Method

A thin compact layer of TiO<sub>2</sub> nanoparticles (~40 nm) was coated onto fluorine-doped tin oxide (FTO) glass by spin coating Ti(IV) bis(ethyl acetonato)-diisopropoxide solution (i.e., sol-gel hydrolysis) and was then calcined to 500 °C for 10 minutes, which prevented direct contact of the electrolytes with the FTO glass. Then, a square-shaped PDMS mold was placed on an FTO glass substrate and was assembled by it clamping together. The mold was then used as a solution reservoir. A mixture of PS microspheres and synthesized TiO<sub>2</sub> nanoparticles were prepared in water, and several drops of the mixture were added into the PDMS mold on FTO glass. Then, the mixture was left to dry slowly at room temperature under high relative humidity (ca. 90–95%), and the PDMS mold was detached carefully. After removing sacrificial PS microspheres at high or low temperature (a thermal calcination or a solvent soaking method), TiO<sub>2</sub> film was immersed at room temperature in a 0.5 mM solution of purified N719 dye in anhydrous ethanol for 12 hr. A Pt counter electrode was prepared by spin coating a 0.7 mM H<sub>2</sub>PtCl<sub>6</sub> solution and was heated at 400 °C for 15 min. Both electrodes were sealed with 25 μm surlyn as a spacer between electrodes. After sealing, the liquid electrolyte was injected through two holes predrilled into the counter electrode.

The schematic diagram in Figure 2 illustrates the experimental procedure for fabricating the DSSCs used in this study. A macroporous structure was produced after drying a mixture of polymer microspheres and titania nanoparticles on FTO glass. In order to remove the sacrificial template PS microspheres, there were two methods at different temperatures (high or low temperature). As a high-temperature process (HT process, Fig. 2(a)), the dried film was calcined in air at 500 °C for two hours at a heating rate of 4 °C/min, and the removal of PS microspheres left behind air cavities within a titania structure. Another way was at low temperature (LT process, Fig. 2(b)), where the dried film was compressed at 70 °C for 2 min due to increased contact between a substrate and a film. Then, this film was baked in air at 150 °C for two hours in order to interconnect TiO<sub>2</sub> nanoparticles. Subsequently, the film was soaked in chloroform solvent to remove PS microspheres.

### 2.3. Characterization of TiO<sub>2</sub> Photoelectrodes

Figure 3 shows SEM images of the macroporous TiO<sub>2</sub> films structure fabricated after removing PS colloid particles at high or low temperature, respectively. In Figures 3(a–c), PS particles were removed by thermal treatment at 500 °C. In Figures 3(d–f), they were successfully removed by soaking in solvent and baked softly at 150 °C. Usually, after thermal calcinations using TiO<sub>2</sub>

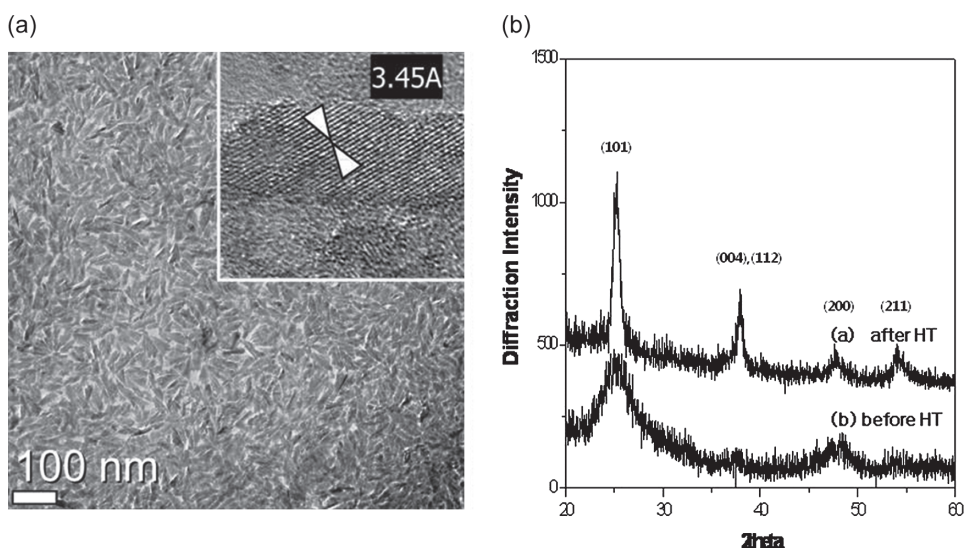


**Fig. 1.** Characterizations of TiO<sub>2</sub> particles synthesized in this study: (a) TEM images and (b) X-ray diffraction patterns of the TiO<sub>2</sub> films.

precursors (i.e., sol-gel process) within the polymeric colloidal array, severe volume contraction was found due to the generation of water molecules. These contribute to a decrease of the efficient cell area or poor contact between TiO<sub>2</sub> films and the substrate in DSSCs. Even though we used pre-synthesized TiO<sub>2</sub> nanoparticles, the residual waters escaped during thermal treatment, and some cracks were generated within TiO<sub>2</sub> film (Fig. 3(a)). However, the cracks were not severe compared to those which were

found in usual sol-gel process using TiO<sub>2</sub> precursor. During the solvent evaporation at high temperature, the shear force by solvent flow was generated near the surface. Subsequently, the pore ordering on the upper side of TiO<sub>2</sub> film was observed to be better than that of the bottom side. In the case of macroporous structures treated by solvent at low temperature, significant cracks were not found and the ordering of pores was disrupted overall, as shown in Figures 3(d-f). In order to confirm the elimination of polymer particles by soaking in solvent, the concentration of carbon particles in TiO<sub>2</sub> film was monitored by a field emission-electron probe micro analyzer (FE-EPMA, JXA-8500F). The concentration of carbon component was 0.192 wt% in the HT process and 1.519 wt% in the LT process. The tiny values indicate that the polymer particles were successfully removed, and it did not significantly affect the solar cell performance.

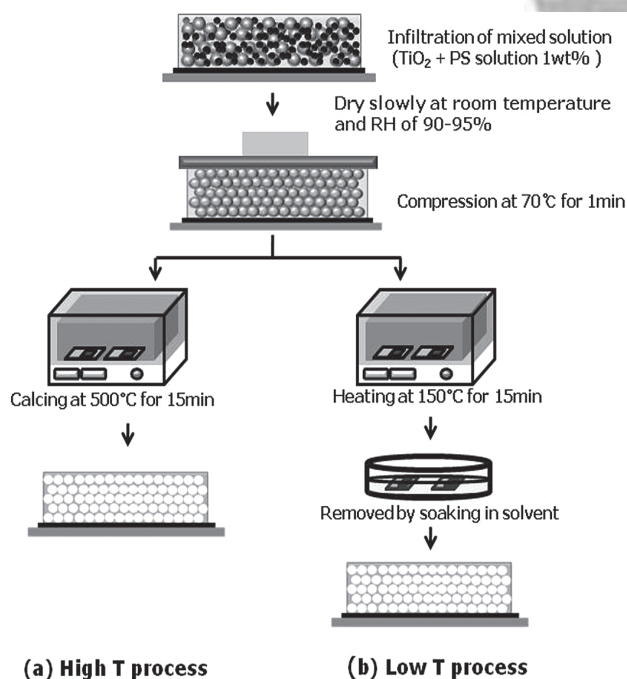


**Fig. 2.** Schematic diagram showing the co-sedimentation of TiO<sub>2</sub> nanoparticles and polymeric particles to fabricate macroporous TiO<sub>2</sub> photoelectrodes using (a) high temperature process-thermal calcination, (b) low temperature process- solvent soaking method.

#### 2.4. Solar Cell Performance

The cell performance is shown in Figure 4. Their photocurrent density-voltage characteristics and the related physical values such as  $\eta$  (light-to-electricity conversion efficiency),  $J_{sc}$  (short circuit current),  $V_{oc}$  (open circuit voltage), and FF (fill factor) are presented in an inset in Figure 4. In previous reports, compact inverse-opal (IO) electrodes were fabricated by infiltrating non-aggregated TiO<sub>2</sub> nanoparticles into PS colloidal self-assembled template, and the cell efficiencies were reported to be as high as 3.47% under AM 1.5 illumination.<sup>14</sup> These values were quite high for an IO-structured electrode with a low fraction of TiO<sub>2</sub> in an electrode; the maximum volume fractions occupied by TiO<sub>2</sub> should be 26% if IO film is assumed to have a perfect faced center cubic packing structure. Practically, the TiO<sub>2</sub> fraction was much lower



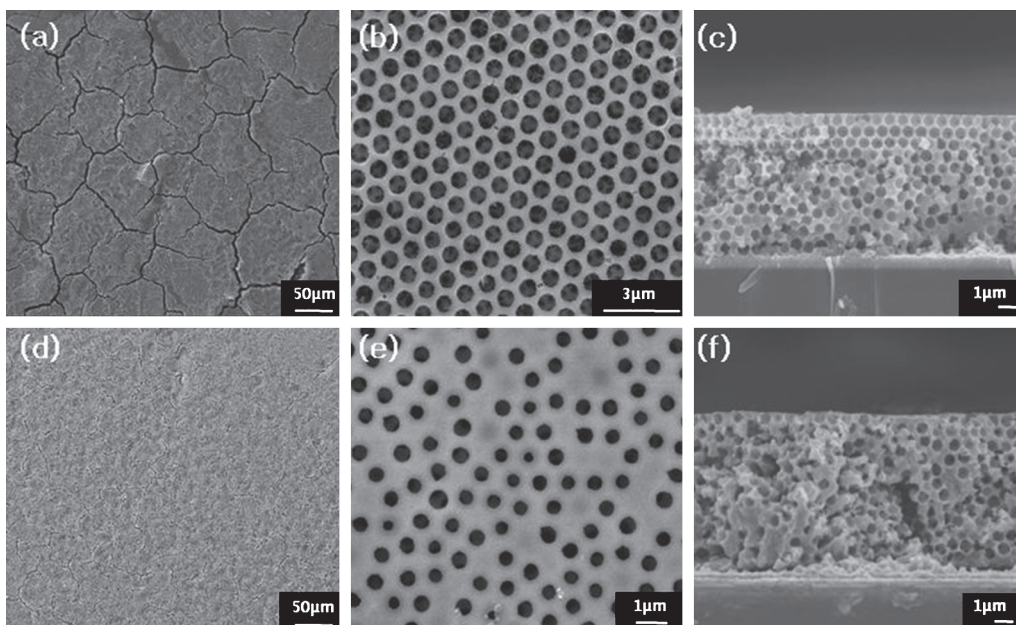


Fig. 3. SEM images of macroporous TiO<sub>2</sub> film structures treated (a–c) using the high-temperature (HT) process and (d–f) using the low-temperature process.

Korea Institute of Science & Technology (KIST)  
 IP: 161.122.37.51  
 Mon, 16 Jul 2012 05:58:19

than 26% due to the imperfect infiltration of TiO<sub>2</sub> nanoparticles. In this study, the TiO<sub>2</sub> fraction was kept high by controlling the mixing ratio of the well-dispersed mixture of TiO<sub>2</sub> nanoparticles and PS colloid particles. It increased up to 40% (v/v), and the resultant conversion efficiency was found to be as high as 6.49% for thermal-sintered photoelectrodes. The total film thickness was 12 μm, which was the same as that of the previous TiO<sub>2</sub> photoelectrode templated from the PS colloidal array.<sup>14</sup> Using the same mixture, TiO<sub>2</sub> photoelectrodes were treated using LT process, and the corresponding cell efficiency was 2.25% for a 9 μm-thick TiO<sub>2</sub> film. In spite of the absence of

thermal sintering at high temperature, the TiO<sub>2</sub> particles used in this study provide high crystallinity by the peptization process and the subsequent hydrothermal reaction. In order to increase an intact interfacial contact between the blocking layer and the bottom of the TiO<sub>2</sub> structure and facile electron transport throughout the interconnected TiO<sub>2</sub>, the hot press procedure was added during baking at low temperature.

### 3. CONCLUSION

In conclusion, a novel fabrication method for TiO<sub>2</sub> photoelectrodes was developed using a highly-dispersed solution of TiO<sub>2</sub> nanoparticles and polymeric particles in water. Polymeric particles were selectively and easily removed by thermal calcinations or soaking in solvent. The use of sub-micron sized polymer particles produced a macroporous structure for viscous or solid state electrolytes. Also, this method provides flexible control in TiO<sub>2</sub> fractions, pore size, and fabrication temperature. A highly-dispersed solution of TiO<sub>2</sub> particles with a high crystallinity and polymer particles would provide a promising solution as a low-temperature process for flexible DSSCs.

**Acknowledgments:** The authors thank Dr. Soonho Lim, Dr. Min Park, Dr. Junkyung Kim and Dr. Heesuk Kim for useful discussions. This work was supported by a National Research Foundation of Korea Grant funded by the Korea Government (MEST) (NRF-2009-C1AAA001-0093049 and R11-2005-048-00000-0). W. Lee acknowledges the partial support by the Korea Research Foundation Grant funded by the Korean Government

RESEARCH ARTICLE

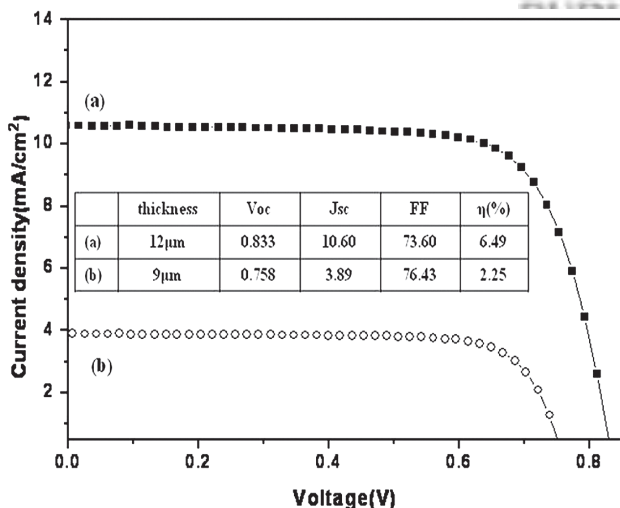


Fig. 4. Current density–voltage characteristics of the macroporous TiO<sub>2</sub> films treated using (a) HT process and treated using (b) LT process, measured at AM 1.5 (100 mW cm<sup>-2</sup>) illumination.

(MOEHRD, Basic Research Promotion Fund) (KRF-2008-331-D00153). This work was supported in part by the 2011 research program of Kookmin University in the Republic of Korea.

## References and Notes

1. X. J. Feng, K. Shankar, O. K. Varghese, M. Paulose, T. J. Latempa, and C. A. Grimes, *Nano Lett.* 8, 3781 (2008).
2. M. Kanungo and M. M. Collinson, *Chem. Commun.* 40, 548 (2004).
3. C. L. Huisman, J. Schoonman, and A. Goossens, *Sol. Energy Mater. Sol. Cells* 85, 115 (2005).
4. P. R. Somani, C. Dionigi, M. Murgìa, D. Palles, P. Nozar, and G. Ruani, *Sol. Energy Mater. Sol. Cells* 87, 513 (2005).
5. X. Fan, F. Z. Wang, Z. Z. Chu, L. Chen, C. Zhang, and D. C. Zou, *Appl. Phys. Lett.* 90, 3 (2007).
6. D. Zhang, T. Yoshida, and H. Minoura, *Adv. Mater.* 15, 814 (2003).
7. G.-S. Kim, H.-K. Seo, V. P. Godble, Y.-S. Kim, O. B. Yang, and H.-S. Shin, *Electrochem. Commun.* 8, 961 (2006).
8. G. Boschloo, H. Lindstr, E. Magnusson, A. Holmberg, and A. Hagfeldt, *J. Photochem. Photobiol. A* 148, 11 (2002).
9. M. Durr, A. Schmid, M. Obermaier, S. Rosselli, A. Yasuda, and G. Nelles, *Nat. Mater.* 4, 607 (2005).
10. X. Liu, Y. Luo, H. Li, Y. Fan, Z. Yu, Y. Lin, L. Chen, and Q. Meng, *Chem. Commun.* 43, 2847 (2007).
11. T. Miyasaka and Y. Kijitori, *J. Electrochem. Soc.* 151, A1767 (2004).
12. N. G. Park, K. Kim, M. Kang, K. Ryu, S. Chang, and Y. J. Shin, *Adv. Mater.* 17, 2349 (2005).
13. K.-M. Lee, C.-W. Hu, H.-W. Chen, and K.-C. Ho, *Sol. Energy Mater. Sol. Cells* 92, 1628 (2008).
14. E.-S. Kwak, W. Lee, N.-G. Park, J. Kim, and H. Lee, *Adv. Funct. Mater.* 19, 1093 (2009).
15. S. Mahshid, M. Askari, and M. S. Ghamsari, *J. Mater. Process. Tech.* 189, 296 (2007).
16. S. Hore, E. Palomares, H. Smit, N. J. Bakker, P. Comte, P. Liska, K. R. Thampi, J. M. Kroon, A. Hinsch, and J. R. Durrant, *J. Mater. Chem.* 15, 412 (2005).
17. Y. G. Seo, H. Lee, K. Kim, and W. Lee, *Mol. Cryst. Liq. Cryst.* 520, 201 (2010).
18. Y. G. Seo, M. A. Kim, H. Lee, and W. Lee, *Sol. Energy Mater. Sol. Cells* 95, 332 (2011).

Delivered by Ingenta to:  
Korea Institute of Science & Technology (KIST)  
IP : 161.122.37.51  
Mon, 16 Jul 2012 05:58:19

Received: 5 November 2010. Accepted: 26 January 2011.

